

# Designing ultra-narrowband interference filters

Sonia Cianci<sup>a,b</sup>, Joss Bland-Hawthorn<sup>b</sup>, John O'Byrne<sup>a</sup>

<sup>a</sup>University of Sydney, NSW 2006 AUSTRALIA

<sup>b</sup>Anglo-Australian Observatory, PO Box 176, Epping NSW 2016 AUSTRALIA

## ABSTRACT

To understand the factors involved in the cost and risk of manufacture of ultra-narrowband imaging filters in the near IR, we have carried out detailed design work for a range of different filter specifications. This work was essential to the success of the DAZLE near-IR imaging spectrograph, a project led by the Institute of Astronomy, University of Cambridge. We find that the necessity for very narrow passbands (approximately 1 nm), for observing through the windows between the OH emission lines in the near-IR bands, required more than 200 layers, leading to coatings of greater than 30  $\mu\text{m}$  thickness. Blocking OH and thermal emission over wide near-IR spectral ranges (1.4 – 2.8  $\mu\text{m}$ ) also required many thin film layers in the filter coatings. In most cases, the large number of layers is the most significant factor in determining manufacturing cost, as such coatings require long periods of time for deposition (days to weeks), and this also increases the risk during manufacture.

**Keywords:** instrumentation: miscellaneous

## 1. INTRODUCTION

DAZLE (Dark Ages Redshift ('z') Lyman Explorer) is an instrumentation project initiated by the Institute of Astronomy (IoA), University of Cambridge, with design performed in collaboration with the Anglo-Australian Observatory. The single aim of this instrument is to detect Lyman- $\alpha$  ( $\text{Ly}\alpha$ ) emitting galaxies in a narrow redshift interval at high redshift ( $7 < z < 10$ ), beyond the limits of current instrumentation – i.e. during the so-called 'Dark Ages'. For an overall discussion of this instrument, see Horton *et al.* (2004).

A crucial component of DAZLE is the filter system, particularly the narrowband filter set, required for wide-field differential images of selected regions of sky. Due to tight specifications required for this instrument, it was important to understand the viability of filter designs and the factors driving the cost of filter manufacture. This was achieved by investigating possible interference thin film designs for the filter system.

### 1.1. $\text{Ly}\alpha$ galaxies at high redshift.

A major area of both observational and theoretical cosmology is the investigation of galaxy formation. Over the past several years, there has been a great deal of progress in this field, with samples of star-forming galaxies being detected at progressively higher redshifts:  $z \sim 1$  (Cowie *et al.* 1996);  $z \sim 3$  (Steidel *et al.* 1996);  $z \sim 4.5$  (Hu & McMahon 1996);  $z \sim 5.7$  (Ajiki *et al.* 2003, Rhoads *et al.* 2003);  $z = 5.74$  (Hu *et al.* 1999);  $z = 6.56$  (Hu *et al.* 2002a,b) and  $z = 6.578$  (Kodaira *et al.* 2003).

It is expected that direct observations of galaxies at the highest redshifts possible (i.e. the youngest galaxies, as they are forming their first stars) will be important for studies of star and galaxy formation. Searching for these objects via detection of the  $\text{Ly}\alpha$  recombination emission line ( $\lambda_0 = 1216 \text{ \AA}$ ) has proven to be an effective technique (e.g. Hu *et al.* 2002, 1999). For higher redshifts, however, it becomes increasingly difficult to detect these objects as the faint  $\text{Ly}\alpha$  line is redshifted further into the near-IR spectral region, where the brightness of the night sky increases steadily (primarily due to OH emission).

## 1.2. Differential imaging for DAZLE

Maihara *et al.* (1993) have shown that in the absence of the OH lines the near-IR sky may actually be darker than the optical sky. High spectral resolution observations (e.g.  $R \sim 1000$ ) can capitalize on this dark near-IR background. This resolution should match the typical expected integrated line width for the high-redshift galaxies of approximately  $100 \text{ km s}^{-1}$ . For such observations, DAZLE will use a pair of very narrowband (FWHM  $\sim 1 \text{ nm}$ ) thin film interference filters, with passbands positioned in one of the dark near-IR windows, but offset slightly in wavelength.

DAZLE will make use of the benefits of differential imaging for wide-field (field of view:  $6.83' \times 6.83'$ ) observations at a particular redshift beyond the sensitivity limits of current instrumentation. Target fields will be chosen on the basis of the deepest possible optical broadband imaging. During an observation, the narrowband filters will be switched repeatedly to produce near-simultaneous images that can be combined differentially. A positive detection of a source in one of the narrow bands which is absent in the other is likely to be a line-emitting source. A lack of (pre-determined) corresponding optical emission suggests that the line emission is Ly $\alpha$  at high redshift – i.e. the positive detection has no corresponding image in the deep pre-existing optical imaging.

The narrowband filters can be designed for imaging at specific wavelengths, or equivalently, at specific redshifts. DAZLE will image in the  $J$  band, where the windows between the OH line emission bands are cleaner compared to the  $I$  band. A narrowband filter pair is planned for operation at  $\sim 1.06 \mu\text{m}$ , which corresponds to a Ly $\alpha$  redshift of around 8.7. After an initial survey at this redshift, another narrowband filter pair may be manufactured for operation at  $z \sim 9.7$  ( $\lambda \sim 1.18 \mu\text{m}$ ).

## 1.3. The DAZLE camera system

DAZLE will use the existing CIRPASS (Cambridge Infra-Red Panoramic Survey Spectrograph; Dean 2002, Parry 2004) camera (Figure 1). The main changes to the CIRPASS camera system will be the inclusion of the DAZLE filters, and a HgCdTe (mercury-cadmium-tellurium) Rockwell HAWAII-2 2K x 2K detector array instead of the current HAWAII 1K detector.

An important requirement for the DAZLE filters is that they sufficiently block unwanted wavelengths over the detector sensitivity range. As well as blocking the OH emission, it is necessary to block the rapidly rising thermal IR emission redward of the  $J$  band. To achieve these specifications, a combination of narrowband and blocking filters will be used. Although this may slightly decrease the total transmission of the narrow passband, the number and total thickness of coating layers is significantly lower than for a single filter, thus reducing the risk and cost of manufacture.

The camera will be cryogenically cooled using liquid nitrogen (77 K), to reduce thermal IR emission from the optical components and their mounts and maximize the efficiency of the detector. The narrowband filters will be positioned just outside the cryogenic camera chamber, as any thermal emission emitted by these will be blocked by the edge filters in the cryostat. The entire DAZLE instrument will be in a refrigerated unit at a temperature of approximately  $-40^\circ\text{C}$ , to reduce the residual thermal emission from the components outside the CIRPASS camera.

## 2. DAZLE FILTER REQUIREMENTS

DAZLE called for thin film coating design work involving two narrowband filters closely spaced in wavelength, with out-of-band rejection to complement existing CIRPASS blocking filters for suppression of OH and thermal emission. Details are given below.

### 2.1.1. DAZLE Narrowband filters

The narrowband filters are required to isolate the redshift of interest for DAZLE observations. A pair of narrowband filters will be used, with closely spaced central wavelengths, essentially targeting a single redshift. Each passband

requires a FWHM of approximately 1 nm, sharp cut-off, and high rejection (optical depth greater than 4.5) outside the passband in order to minimise leakage from the OH lines, between which the transmission bands lie. The filters are designed for zero tilt (in a collimated beam) and zero wedge to optimise passbands across the full field. Ghosting (due to reflections from the detector and optical components) will be minimal unless there is a very bright object in the field. The narrowband filters will be positioned outside the cryogenic camera chamber, but in a refrigerated unit at approximately  $-40^{\circ}\text{C}$  (233 K), which needs to be considered when designing the thin film coatings (as the optical properties of the coating materials vary with temperature; see Section 7.3). A diameter of 100 mm is required for each filter, to match the size of the entry window into the camera unit.

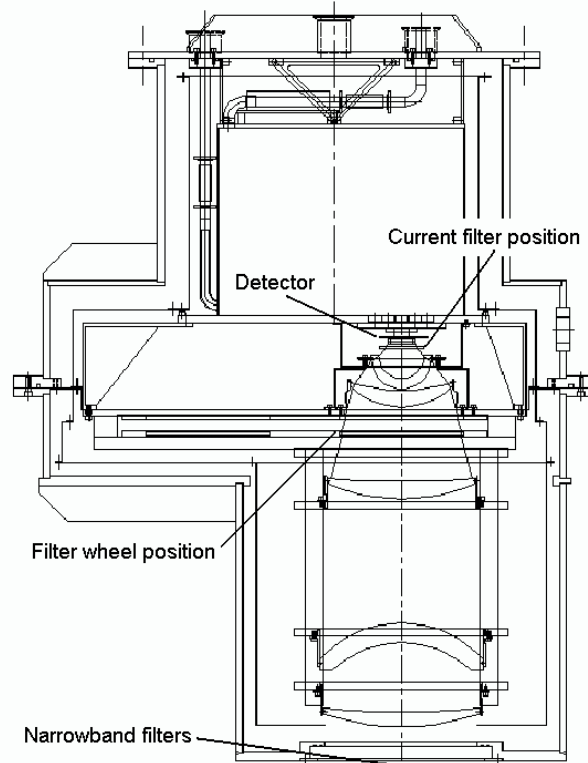


Figure 1. Schematic of CIRPASS camera system in cryogenic chamber. The  $1.8\ \mu\text{m}$  blocking filter position is shown, just in front of the detector. The filter wheel will hold the  $1.4\ \mu\text{m}$  blocking filter, while the DAZLE narrowband filters are to be positioned just outside the input window to the cryogenic chamber.

### 2.1.2. Out-of-band blocking

The narrowband filters will have high rejection outside their passbands, but the complexity of their thin film coatings limits the range of the rejection bands. Blocking filters, combined with the narrowband filters, are therefore essential to remove effects on the background from the thermal IR at longer wavelengths, and visible sources at shorter wavelengths that may saturate the detector.

Transmission is required from  $0.95\ \mu\text{m}$  up to the longest wavelength required to meet the DAZLE science objectives ( $1.334\ \mu\text{m}$  is equivalent to  $z = 10$ ), permitting the use of narrowband pairs up to this limit. Blocking must be effective from  $0.95\ \mu\text{m}$  down to  $0.5\ \mu\text{m}$ , and  $1.35\ \mu\text{m}$  up to  $2.8\ \mu\text{m}$ , beyond which the detector sensitivity has dropped substantially. The OD requirements redward of the *J* band must exceed  $\sim 4.5$  to block the rapidly rising thermal IR.

### 2.1.3. Influence of detector response on filter design

An issue affecting the design of the DAZLE narrowband/blocking filter combination is the precise quantum efficiency (QE) response of the HAWAII-2 detector array within the CIRPASS camera. According to L. Kozlowski (Rockwell), the short end cut-off of the 2.5  $\mu\text{m}$  HAWAII arrays is somewhat variable but there should be very little photoresponse below 800 nm because the CdZnTe (cadmium-zinc-tellurium) buffer layer absorbs below these wavelengths. The upper cut-off is quite sharp, but does also vary between manufacturing runs. Nevertheless, there should not be any response beyond 2.8  $\mu\text{m}$ .

The HAWAII-2 devices produced by Rockwell use molecular-beam-epitaxy-grown material, due to much lower dark current and material uniformity. One reason why the relevant QE curves are not readily available is that they depend on whether a visible response is needed and whether an anti-reflection coating is specified. The standard material does not support visible detection as the thick CdZnTe substrate absorbs all light below 900 nm. Standard devices are not anti-reflection coated so they have maximum QEs of 70 to 75%; AR coatings raise the peak QEs to above 80%. There are substrate-removed devices which respond through the visible with about 60% QE, down to at least 400 nm. These are not conventional HAWAII arrays.

A customised HAWAII array with a cut-off at or below 1.7  $\mu\text{m}$  would greatly simplify both the CIRPASS and DAZLE blocking problem. However, the current DAZLE budget does not support one of these devices, and there is a concern that the red cut-off will lower the transmission at 1  $\mu\text{m}$ . The HAWAII-2 array to be used in DAZLE has a nominal red cut-off at 2.8  $\mu\text{m}$ .

## 3. PRELIMINARY QUOTATION

In June 2001, Barr Associates provided detailed preliminary quotations for narrowband filters based on filter specifications according to the provisional DAZLE design. With the cost quotes, Barr Associates supplied transmission (T) and OD versus wavelength data sheets. An example of the design profiles and cost quotes are shown in Figure 2.

All narrowband items quoted make use of oxide coatings – tantalum pentoxide ( $\text{Ta}_2\text{O}_5$ ) and silicon dioxide ( $\text{SiO}_2$ ) – on a single fused silica substrate (both sides coated). Oxide coatings are hard and robust to variable environments, allowing them to be deposited onto a single substrate. The oxide coatings were considered appropriate for DAZLE, since they would be subjected to temperature changes as the refrigerated and cryogenic systems are cooled.

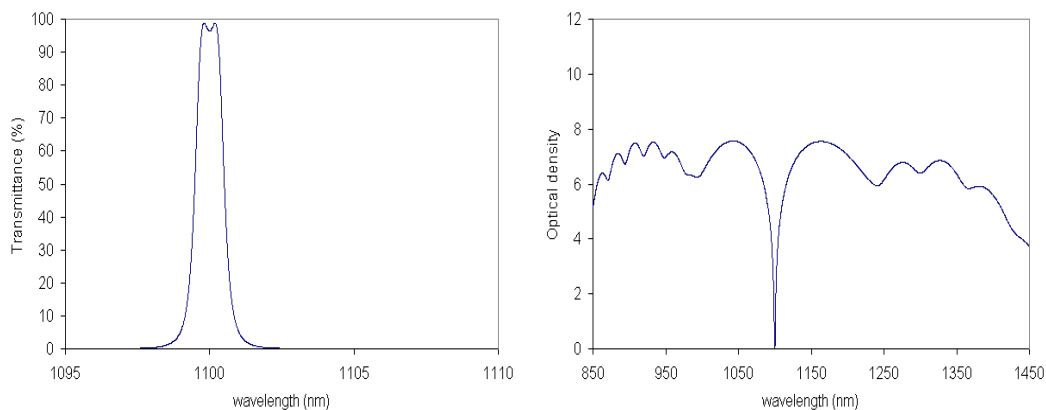


Figure 2. 2-cavity narrowband optical filter design from Barr Associates. *Left*: Designed transmittance profile of the filter, highlighting the passband; *right*: Designed OD profile over the desired operating range of the filter. Quoted specifications: FWHM  $\sim 1.0 \pm 0.2$  nm; central wavelength:  $1100 \pm 0.15$  nm; oxide coatings on a single substrate; peak transmission  $> 75\%$ ; OD  $> 5$  between 0.9  $\mu\text{m}$  and 1.4  $\mu\text{m}$ ; thickness of substrate: 6 mm; operating temperature: 23°C; wedge  $< 30$  arcsec. The cost of this filter using a 2-cavity design was quoted at USD\$28,960.00. A similar filter, using a 3-cavity design, was quoted as costing USD\$46,930.00.

## 4. REVERSE-ENGINEERING FILTER DESIGNS

### 4.1. Why reverse engineer the designs?

The preliminary quotation for filters from Barr Associates guided the planning and design of DAZLE components. Given the great expense of the filters, it was essential to understand which tolerances drive the cost – some tolerances may be relaxed with little impact on the performance but significant impact on cost. Filter companies like Barr Associates, however, guard their secrets well, i.e. they do not disclose their manufacturing prescription.

“Reverse engineering” the designs, i.e. designing thin film coatings using the Barr Associates transmission and OD profiles as targets, provides insights into how the cost depends on the filter parameters specified. This work has led to the knowledge that the DAZLE filters are in the thick coating regime where cost is driven mostly by (i) the coating time in the deposition chamber (measured in days to weeks), (ii) the need to maintain a wide spectral response extending to the blue and the red, and (iii) the filter diameter. Other parameters, such as operating temperature and humidity, affect the performance of the filter but are less important in the cost.

## 5. DAZLE FILTER DESIGN

All designs were produced using *TFCalc*, a commercial thin film software package. *TFCalc* allows the user to enter the materials and thicknesses of thin film coating and substrate, and computes the output optical profile using standard interference theory (for a summary, see Cianci 2003; an extensive description is found in Macleod 2001). The software can also optimise designs by iteratively changing the thicknesses of layers and re-computing the optical profile to more closely match the desired properties of the thin film filter.

### 5.1. Single narrowband filters

Narrow spectral regions between the bright night sky emission lines can be achieved using two-cavity and three-cavity thin film structures. A single cavity with the structure  $(HL)^8 H H (LH)^8$  provides passbands of approximately 1 nm width ( $R \sim 1000$ )<sup>1</sup>, but higher-order cavities were required to produce squarer passbands, as the reduced ‘wings’ at the passband edges minimise the amount of background light leaking into the signal. The materials used in these designs were Ta<sub>2</sub>O<sub>5</sub> ( $n_H \sim 2.15$  at 1  $\mu\text{m}$ ) and SiO<sub>2</sub> ( $n_L \sim 1.48$ ), as used by Barr Associates in their preliminary designs. The passband of the three-cavity structure includes prominent peaks, which were reduced by including a low-order cavity, *HLHHLH*, on either side of the three-cavity structure.

The end results of the two-cavity and three-cavity narrowband filter designs are shown in Figure 3. The final order for filters placed with Barr Associates was for a two-cavity design, as this required fewer layers without greatly affecting the square shape of the passband. The total physical thickness of the coatings for the two-cavity narrowband filter is approximately 30  $\mu\text{m}$  (as opposed to around 40  $\mu\text{m}$  for the three-cavity design).

The passbands of the pair of filters were offset slightly in wavelength for differential comparison of images. The wavelengths chosen for the passbands were 1.0565  $\mu\text{m}$  and 1.063  $\mu\text{m}$ . The two bands are achieved with the same thin film design for each filter, but by simply adjusting the reference wavelength of the design (or monitoring wavelength during manufacture) so that the physical thickness of the layers scales accordingly.

The multiple-cavity structure itself provides very high OD ( $> 8$ ) just around the passband, but the rejection is only of limited extent. The out-of-band suppression was extended to beyond 1.4  $\mu\text{m}$  by combining the multiple-cavity with a broadband filter, which itself required several quarter-wave stacks designed such that their rejection bands overlap, as follows:

$$0.71(0.5HL0.5H)^{20} 0.836(0.5HL0.5H)^{20} 1.192(0.5HL0.5H)^{20}$$

---

<sup>1</sup> The symbols *H* and *L* are used in thin film design as a shorthand notation for quarter-wave layers of high and low refractive index, respectively (relative to the index of the substrate).

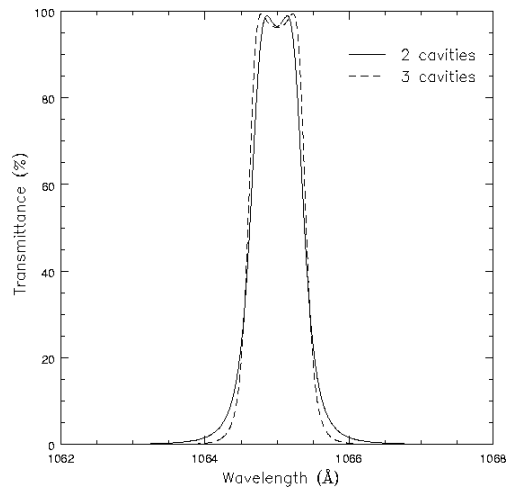


Figure 3. Transmission profiles of 2-cavity (solid line) and 3-cavity (dashed line) DAZLE narrowband filter designs.

(for a reference wavelength of 1.065  $\mu\text{m}$ ). The multiple-cavity design would be deposited on one side of the substrate, and the broadband, extended-rejection filter deposited on the other side. The quarter-wave broadband structure provides suppression on the red side of the narrowband up to  $\sim 1.55 \mu\text{m}$ , to overlap with an edge filter included in the DAZLE instrument.

The spectral range of out-of-band suppression was limited on the blue side of the narrowband by the substrate, for which a filter glass could be used to block optical wavelengths down to around 500 nm (shorter wavelengths would be cut off by the detector edge). Schott Filter Glass RG850 appears to provide a suitable cut-off edge for the DAZLE narrowband filters.

## 6. RESULTS OF FILTER DESIGN

Table 1 summarises the main features of the narrowband filter designs, including the optical density (OD) constraints, the total number of layers and physical thickness of the thin film coatings (i.e. the sum of the number and thickness of layers on the front and back sides of the substrate) for each filter. Figure 4 shows the transmission and OD profiles of the 2-cavity design listed in Table 1, for comparison with the Barr Associates design in Figure 2.

Table 1. Summary of DAZLE narrowband filter designs

Number of cavities	Central wavelength $\lambda_c$ ( $\mu\text{m}$ )	FWHM (nm)	Rejection outside narrowband		OD of rejection regions	Total number of thin film layers	Total thickness of coatings ( $\mu\text{m}$ )
			blue edge ( $\mu\text{m}$ )	red edge ( $\mu\text{m}$ )			
2	1.065	$\sim 1$	$\sim 0.75$	$\sim 1.4$	$> 5$	209	31.8
3	1.065	$\sim 1$	$\sim 0.75$	$\sim 1.4$	$> 5$	255	39.3

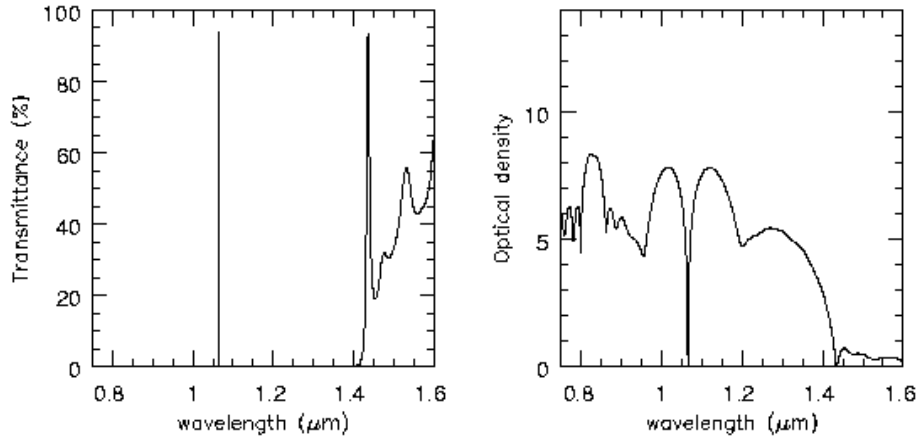


Figure 4. Transmission (left) and OD (right) profiles of the DAZLE narrowband filter design using a 2-cavity thin film structure. This filter needs high rejection only to around 1.4 μm, as it will be used in combination with the DAZLE blocking filters.

## 7. ISSUES RAISED DURING FILTER DESIGN

### 7.1. Filter substrates.

All filters were designed using a fused silica substrate of thickness 6 mm, with the thin film layers distributed on both sides of the substrate. This thickness was taken from the substrate specifications provided in the filter quotes from Barr Associates. BK7 and other materials are possible for use as substrates, but Barr Associates do not guarantee the final transmitted wavefront with these substrates.

A filter glass is to be used as a substrate for the narrowband filters, which will block light blueward of the desired transmission bands. The cut-off edge depends on the type of filter glass used. According to data from Schott Glass, their filter glasses provide an OD > 5 on the blue side of the cut-off edge for 3 mm thick substrates – for a thicker substrate, its blocking OD will increase. A filter glass simplifies the thin film coatings required to block down to the blue cut-off edge of the detector. There may be a slight decrease in the passband transmission due to the filter glass, however the coating design may be able to accommodate this. The optical information required by *TFCalc* to include the filter glass as a substrate is not available, and so only the fused silica substrate was used in the designs. The effects of using the filter glass could be simulated by multiplying the transmission profile of the thin film filter design with that of the filter glass.

### 7.2. Field effects and sky flatness

The imaged field through an interference filter in a collimated beam is not strictly monochromatic. There is a phase effect across the field, which can be derived using the equation of interference:

$$m\lambda = 2nd \cos \theta \quad (1)$$

This equation describes the interference between two reflecting surfaces, i.e. a Fabry-Perot (FP) cavity, where  $m$  is the order of interference,  $n$  and  $d$  are, respectively, the refractive index and thickness of the spacer material for the FP cavity, and  $\theta$  is the transmitted angle of light of wavelength  $\lambda$ . A thin film interference filter, however, comprises multiple FP cavities in series. Thus Equation 1 becomes

$$\lambda = p \cos \theta \quad (2)$$

where  $p$  is a weighted mean of  $N$  interference layers of  $n_i$  and  $d_i$  ( $i = 1 \dots N$ ). This angular dependence of  $\lambda$  leads to a decrease in observed wavelength at the edge or corner of the detector compared with that at the centre of the detector.

What is seen across the detector as a function of physical angle  $\theta$  is a convolution of the filter profile,  $F(\lambda) = F(p \cos\theta)$ , and the sky spectrum,  $S(\lambda) = S(p \cos\theta)$ . So, as a function of wavelength, DAZLE sees

$$D(\lambda) = \int_{\lambda_-}^{\lambda_+} S(\lambda)F(\lambda - \lambda_0)d\lambda_0 \quad (3)$$

where  $\lambda_- = \lambda_0 - \Delta\lambda_N/2$  and  $\lambda_+ = \lambda_0 + \Delta\lambda_N/2$  and  $\lambda_0$  and  $\Delta\lambda_N$  are the central wavelength and the FWHM of the narrowband interference filter. This convolution is shown in Figure 5. The OH spectra (which are not flux calibrated) used in these simulations are taken from Rousselot *et al.* (2000).

Across the detector, DAZLE sees a function of  $\theta$ :

$$D(\theta) = D(u) = \int_{u_-}^{u_+} S(u)F(u - u_0)du_0 \quad (4)$$

where  $u = \cos^{-1}(\lambda/p)$ . An important conclusion is that the clear windows in the OH spectrum observed at high resolution are somewhat narrower when seen through the interference filter.

The DAZLE filter specifications recommend two high priority windows for investigation, at around 1.06  $\mu\text{m}$  and 1.18 – 1.19  $\mu\text{m}$ , which provide spectral regions suitable for positioning of the narrowband filters. Accounting for the field effect described above, it was necessary to select the central wavelengths of the narrowband filters to prevent (or minimise) the filter bandpasses overlapping with any OH spectral lines. For each window, the three most suitable wavelengths were chosen for possible narrowband filter centres (an example is seen in Figure 5).

With the convolved sky spectrum narrowing due to the width of the narrowband filter, the best spectral positions for the narrowband filter pair were found to be at A and B for the 1.06  $\mu\text{m}$  window (see Figure 5), which are slightly wider than the dark windows in the 1.18 – 1.19  $\mu\text{m}$  window. The final selections of central wavelengths for the DAZLE narrowband filter pair were, therefore, at positions A and B (1.0565  $\mu\text{m}$  and 1.063  $\mu\text{m}$ , respectively).

The angle variations due to the field effect are not significant with respect to the blocking filters, as the specific wavelengths of the blocking cut-off edges are not so dependent on the spectral positions of the OH lines.

### 7.3. Temperature effects

Variations in temperature during the use of thin film filters can cause the transmission profiles of the filters to shift significantly in wavelength. The shift is mainly due to the change in refractive index of the materials. In general, narrowband filters are the most affected. For most thin film filters, there is a shift in the maximum transmission towards shorter wavelengths with decreasing temperature. The variation in the maximum position is affected by the wavelength of operation and the method of deposition, and also varies between filters from different manufacturers. For materials commonly used in the visible region of the spectrum, the shift is of the order  $0.003\% \lambda \text{ K}^{-1}$  ( $\sim 0.3 \text{ \AA K}^{-1}$  at 1.06  $\mu\text{m}$ ), while for infrared filters a useful figure is  $0.005\% \lambda \text{ K}^{-1}$  ( $\sim 0.5 \text{ \AA K}^{-1}$  at 1.06  $\mu\text{m}$ ).

Some studies show that for bandpass filters, there is little loss of peak transmittance or variation of characteristic passband shape down to liquid helium temperatures.

Since the DAZLE narrowband filters are to operate at a temperature of  $\sim 230 \text{ K}$ , their passbands will shift  $\sim 1.5 \text{ nm}$  bluewards of the passbands created during manufacture (at room temperature). It is, therefore, necessary to account for this shift in the thin film design, and actually manufacture the filters with passbands slightly higher in wavelength than those specified. Barr Associates guarantee that the filters they manufacture will perform at the correct wavelengths at the specified operating temperature.



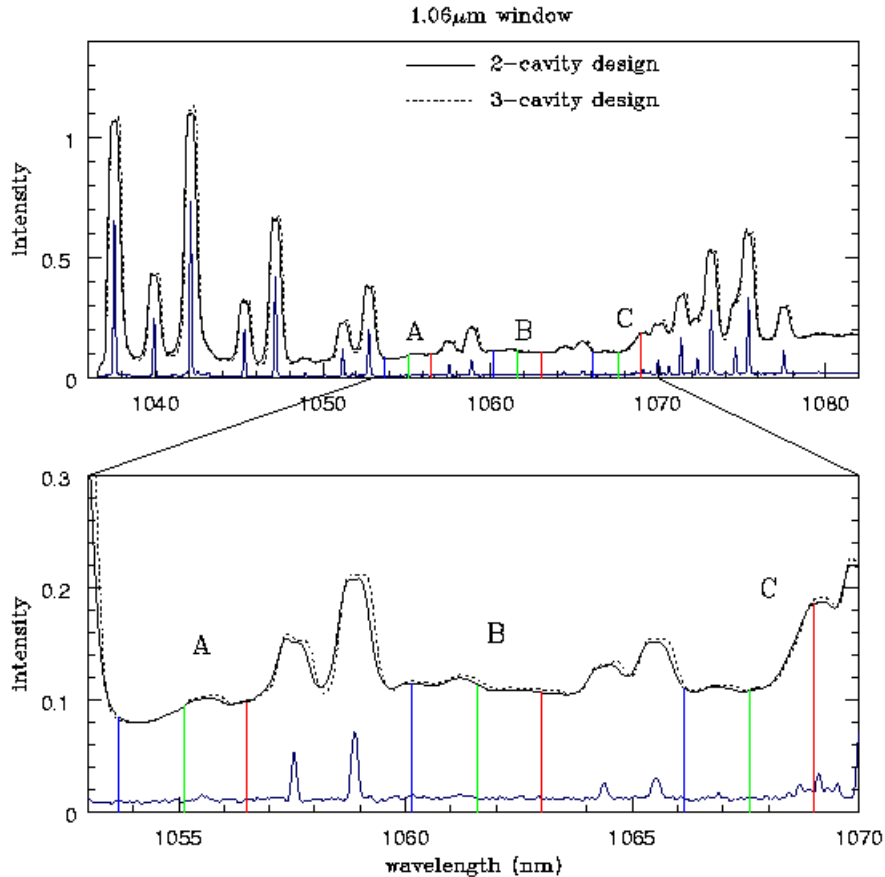


Figure 5. OH sky spectrum (Rousselot *et al.* 2000) for the 1.06  $\mu$ m window (solid dark blue line), and the same spectrum convolved with the DAZLE 2-cavity (solid black line) and 3-cavity (dotted line) narrowband filter profiles. A, B and C indicate possible spectral positions for the narrowband filters, with the red lines corresponding to the central wavelengths at the centre of the DAZLE field. The green and light blue lines correspond to the shifted central wavelengths observed at the edge and corner of the detector, respectively. The bottom plot highlights the region of the top plot with the possible filter positions.

## 8. STATUS OF PROJECT

This filter design work was performed as part of the Concept Design phase of the DAZLE project. The AAO carried out the optical and mechanical design of the collimator for the instrument, which was completed in late 2003. DAZLE is currently well into the manufacturing phase at the IoA, with most of the key optical and mechanical components ready for assembly (see <http://www.ast.cam.ac.uk/~optics/dazle/photos/>). The filter wheel and mask wheel assembly was completed in October 2003.

The first narrowband filter was manufactured by Barr Associates and delivered in August 2003. The width of the passband of this filter is measured at approximately 1 nm, centred at 1.05  $\mu$ m, which meets the optical specifications. The out-of-band suppression is also adequate for the planned observations. Although the peak transmission, at approximately 65%, is notably less than desired, the IoA accepted this filter, and Barr Associates are currently manufacturing the second narrowband filter for DAZLE.

It is hoped that DAZLE will go to the Very Large Telescope for commissioning in 2005. Initial plans are for a 4-year science exploitation phase, with the possibility of obtaining another filter set in the future, for detection of galaxies by searching for red-shifted Ly $\alpha$  at around 1.18  $\mu\text{m}$  ( $z = 8.8$ ).

## REFERENCES

1. Ajiki, M., Taniguchi, Y., Fujita, S.S., Shioya, Y., Nagao, T., Murayama, T., Yamada, S., Umeda, K. & Komiyama, Y. 2003, *AJ*, **126**, 2091 – 2107
2. Cowie, L. L., Songaila, A., Hu, E. M. & Cohen, J.G. 1996, *AJ*, **112**, 839 – 864
3. Dean, A. *CIRPASS: The Cambridge Infrared Panoramic Survey Spectrograph*, PhD thesis, Institute of Astronomy, University of Cambridge, 2002
4. Horton, A., Parry, I., King, D., Medlen, S., McMahon, R. & Sharp, R. 2004, *Proc. SPIE*, **5492**
5. Hu, E.M., Cowie, L.L., McMahon, R.G., Capak, P., Iwamuro, F., Kneib, J.-P., Maihara, T. & Motohara, K. 2002a, *ApJL*, **568**, L75 – L79
6. Hu, E. M., Cowie, L.L., McMahon, R.G., Capak, P., Iwamuro, F., Kneib, J.-P., Maihara, T. & Motohara, K. 2002b, *ApJL*, **576**, L99
7. Hu, E. M. & McMahon, R. G. 1996, *Nature*, **382**, 231 – 233
8. Hu, E. M., McMahon, R. G. & Cowie, L. L. 1999, *ApJL*, **522**, L9 – L12
9. Kodaira, K. *et al.* 2003, *PASJ*, **55**, L17 – L21
10. Parry, I. 2004, *Proc. SPIE*, **5492**
11. Rhoads, J.E., Dey, A., Malhotra, S., Stern, D., Spinrad, H., Jannuzi, B.T., Dawson, S., Brown, M.J.I. & Landes, E. 2003, *AJ*, **125**, 1006 – 1013
12. Rousselot, P., Lidman, C., Cuby, J.-G., Moreels, G. & Monnet G. 2000, *A&A*, **354**, 1134 – 1150
13. Steidel, C. C., Giavalisco, M., Pettini, M., Dickinson, M. & Adelberger, K. L. 1996, *ApJL*, **462**, L17 – L21